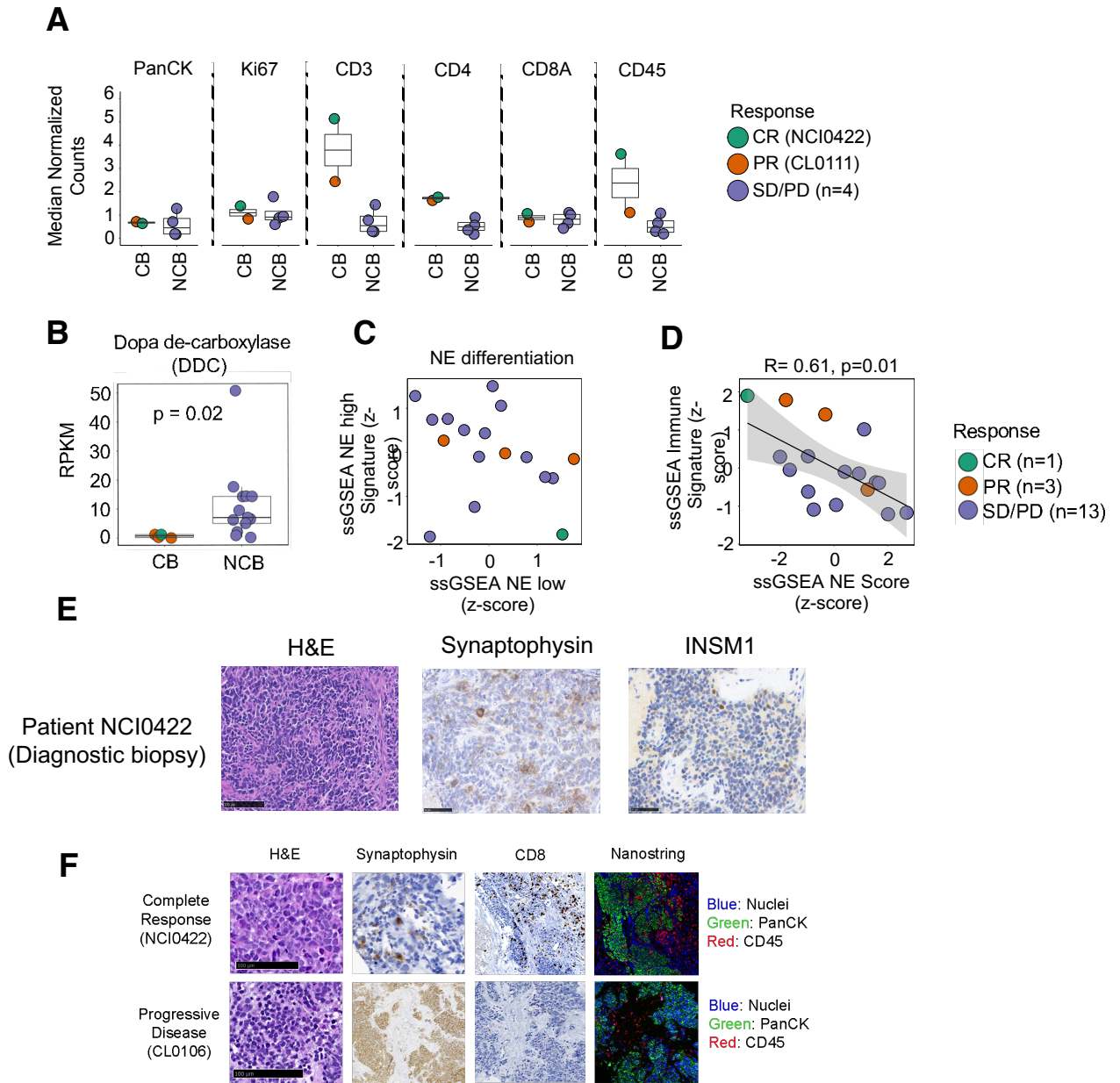
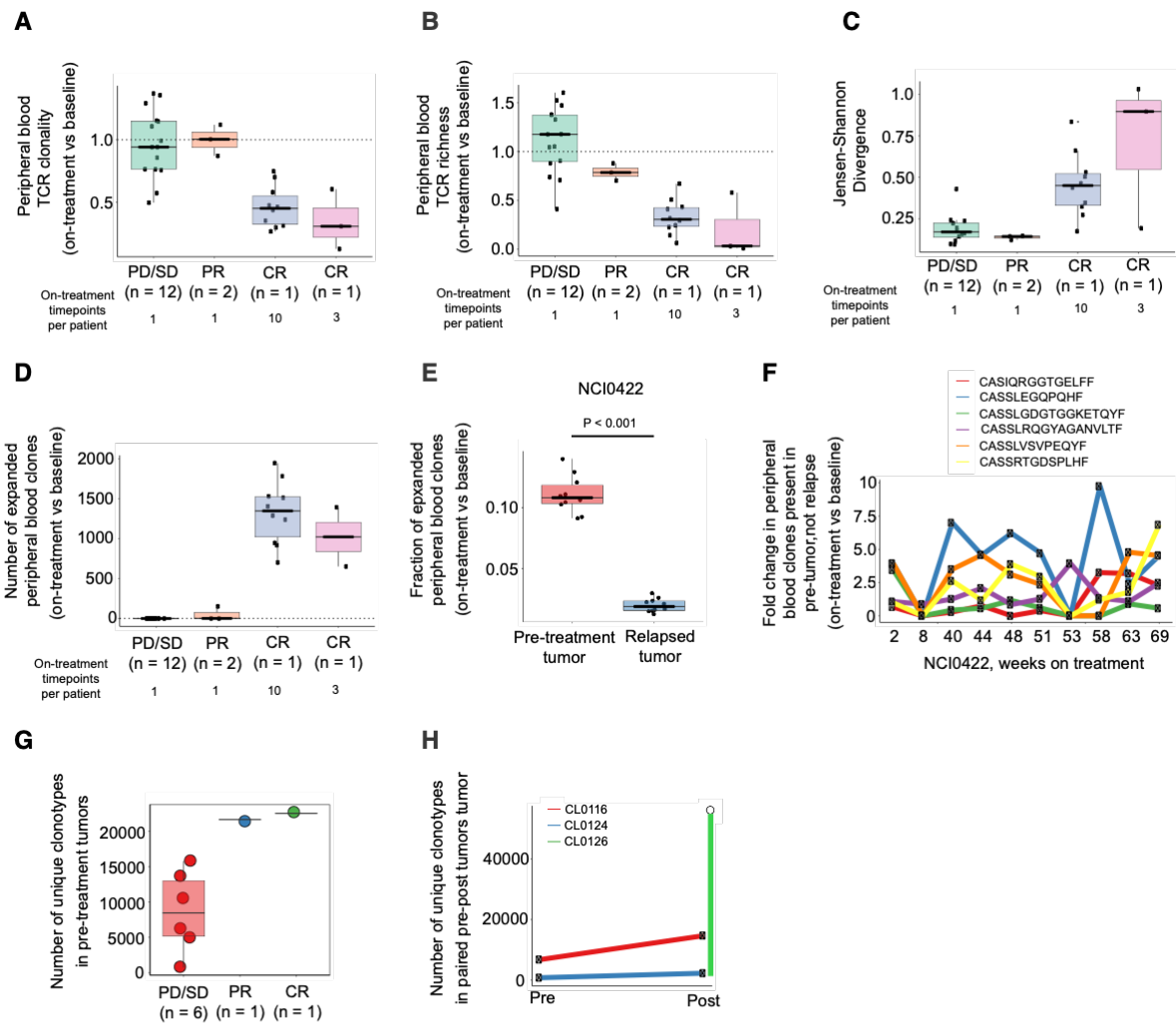


**Figure S1: H&E images of tumors in NCI discovery cohort of patients treated with combination ICB.** Tumor IDs are listed to the left of each H&E image. Scale bars, 50  $\mu$ m. H&Es for CL0114 and CL0147 are not shown.



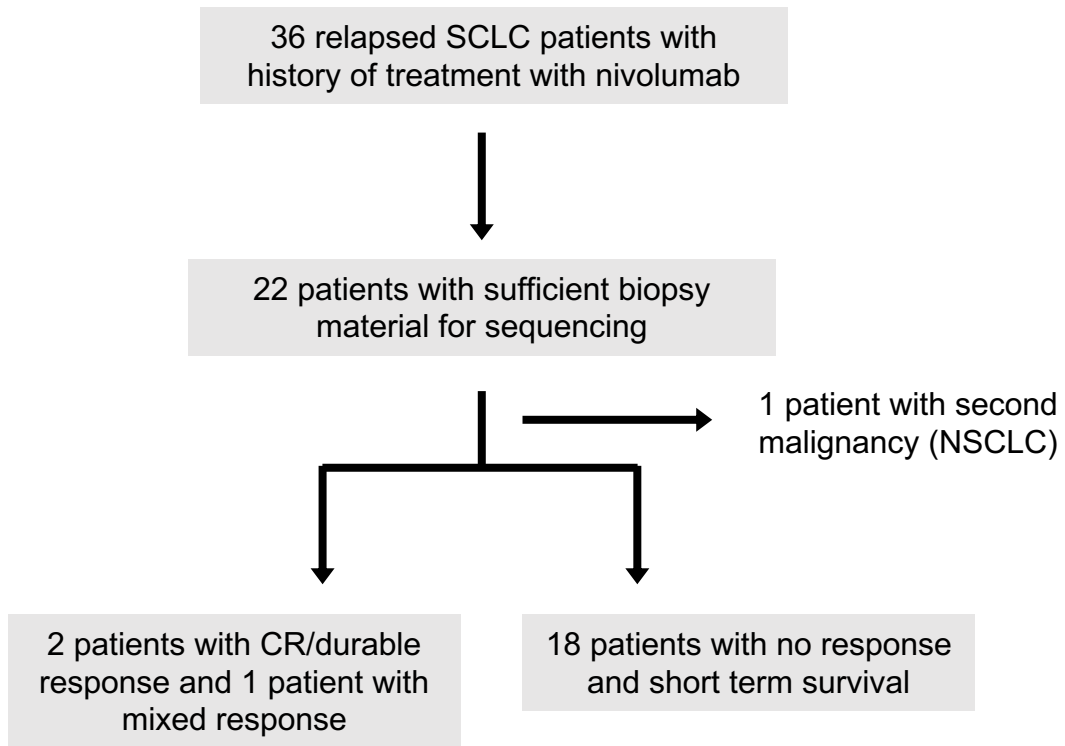
**Figure S2: Transcriptomic and immunohistochemical markers of tumor immunity and neuroendocrine differentiation among NCI discovery cohort patients treated with combination ICB.** (A) Digital spatial profiling of B and T-cell antigens in tumors of patients with and without CB to ICB. (B) Expression of NE gene dopa de-carboxylase (*DDC*) in tumors of patients with CB and NCB. (C) ssGSEA NE differentiation scores of all tumors. (D) Correlation between ssGSEA NE differentiation and immune gene set scores across all tumors. 95% confidence interval for the line shown in grey shading. (E) IHC staining for synaptophysin and INSM1 are shown for a diagnostic biopsy in patient NCI0422. Scale bars, 100  $\mu$ m for H&E and 50  $\mu$ m for synaptophysin and INSM1. (F) H&E, Synaptophysin and CD8 IHC for a patient with complete response (NCI0422) and a patient with progressive disease (CL0106). Scale bars, 100  $\mu$ m Digital spatial profiling (Nanostring) image is also shown. Statistical significance was tested with a two-tailed Mann–Whitney U-test. Blue: Nuclei; Green: PanCK; Red: CD45. Boxplots represent the median, 25th and 75th percentiles and the vertical bars span the 5th to the 95th percentiles. Source data are provided as a Source Data file



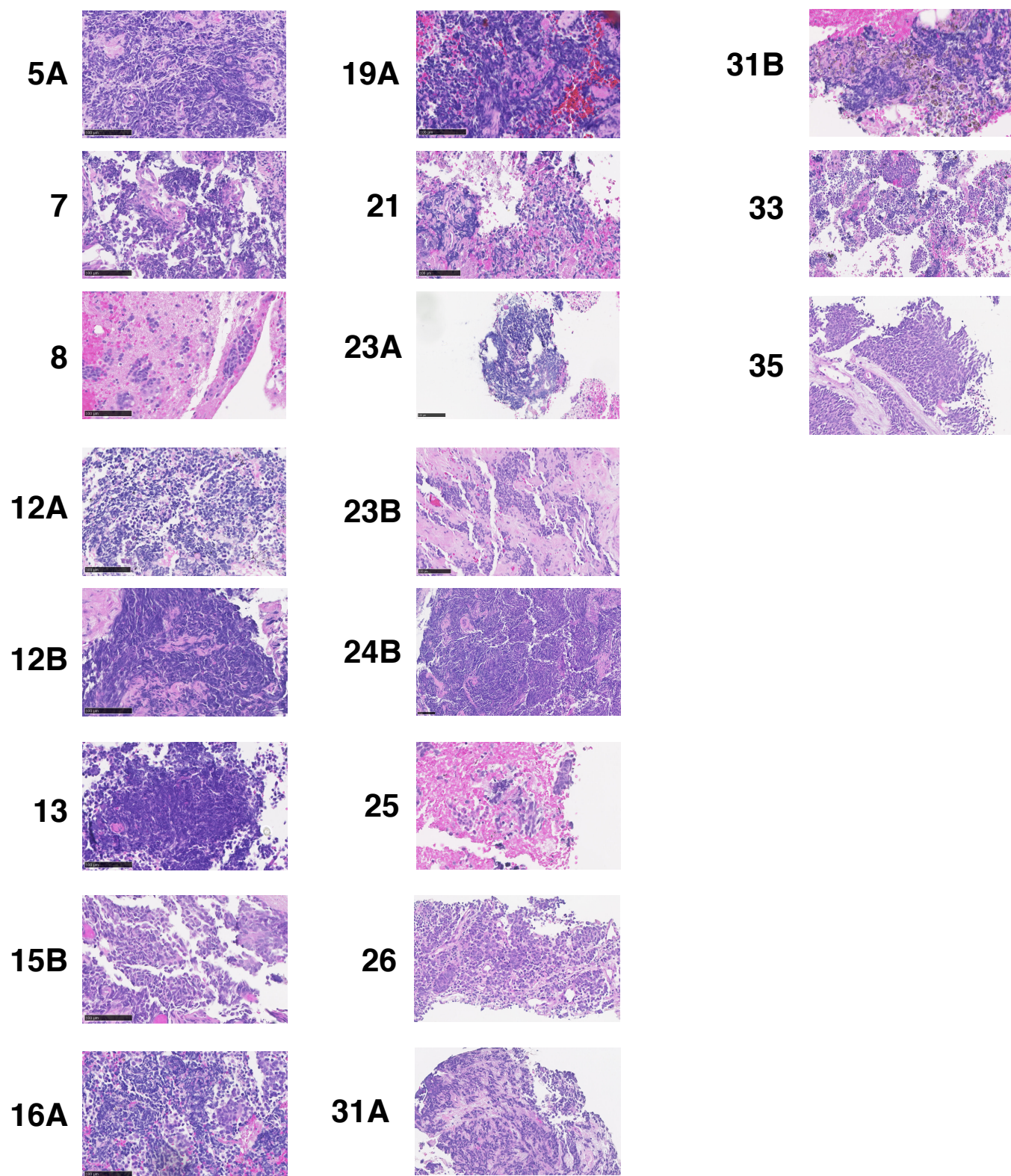


**Figure S3: Alterations in peripheral blood T-cell repertoire and T-cell clonotype expansion are associated with clinical benefit to combination ICB in NCI discovery cohort.** Fold change in peripheral blood T-cell receptor **(A)** clonality, **(B)** richness, and **(C)** Jensen-Shannon Divergence in on-treatment with combination ICB versus pre-treatment samples. Patients are stratified by response. Additional on-treatment timepoints (blue box plots) and an alternative RNA-based TCR-seq (pink box plots) were analyzed for patient NCI0422 (CR). Dotted black line indicates no change. **(D)** Number of expanded peripheral blood clones between on-treatment and pre-treatment samples. Expanded clones are defined as unique, productive clonotypes with fold change greater than 3 and greater than 10 total reads from TCR-sequencing of peripheral blood. **(E)** Fraction of expanded peripheral blood clones from each timepoint of patient NCI0422 present in pre-treatment tumor and tumor at relapse. **(F)** Fold change in expanded peripheral blood clones of patient NCI0422 across multiple timepoints present in the pre-treatment tumor but not in the tumor at relapse. CDR3 amino acid sequences for each of the six peripheral blood clones are shown. **(G)** Number of unique, productive clonotypes within pre-treatment tumor biopsies. Boxplots represent the median, 25th and 75th percentiles and the vertical bars span the 5th to the 95th percentiles. **(H)** Number of unique, productive clonotypes in paired pre-post tumors. Post only tumor is shown for patient CL0126 (PR). Statistical significance was tested with a two-tailed Mann–Whitney U-test (unadjusted p-values shown). PD: progressive disease; SD: stable disease; PR: partial response; CR: complete response. Source data are provided as a Source Data file.

## Rochester Cohort

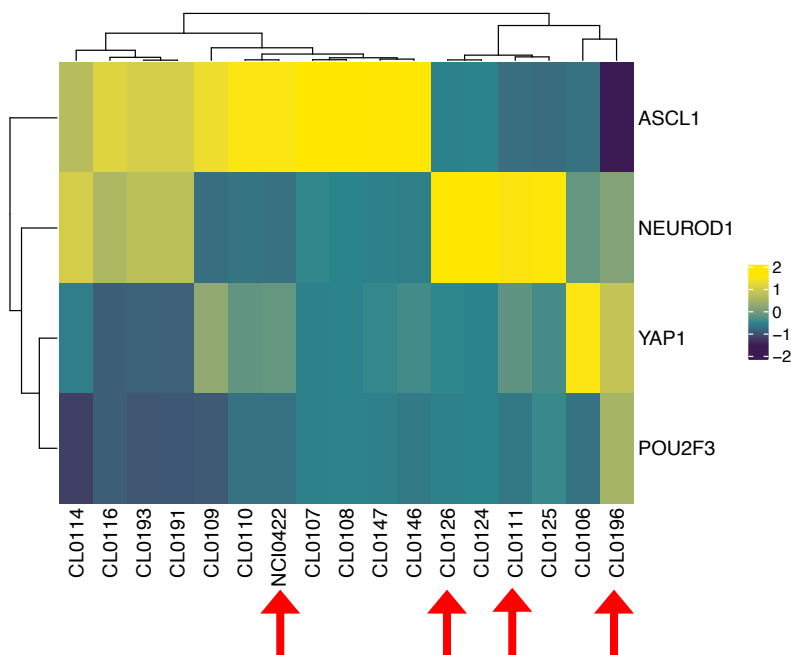
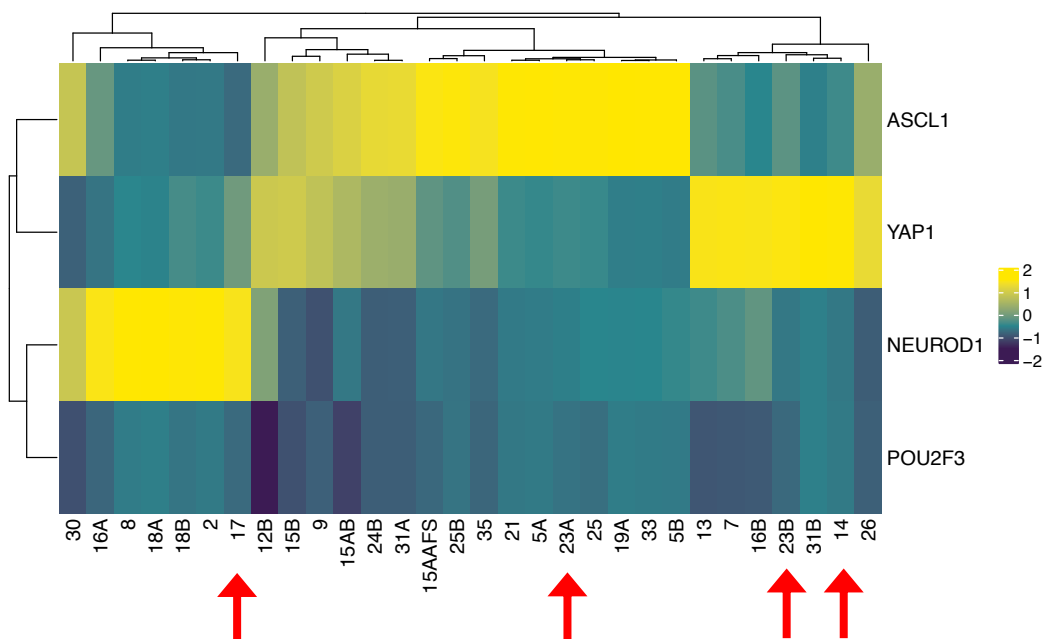


**Figure S4: Flow diagram of samples from the Rochester validation cohort of relapsed SCLC patients treated with ICB.**

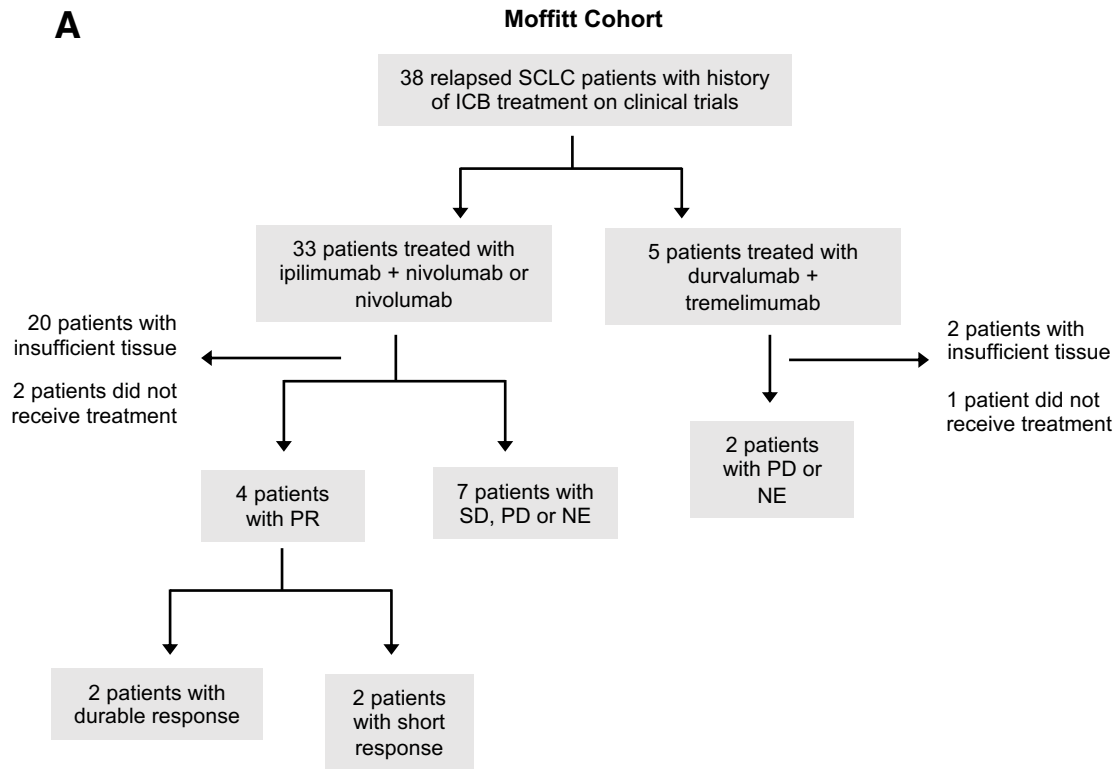
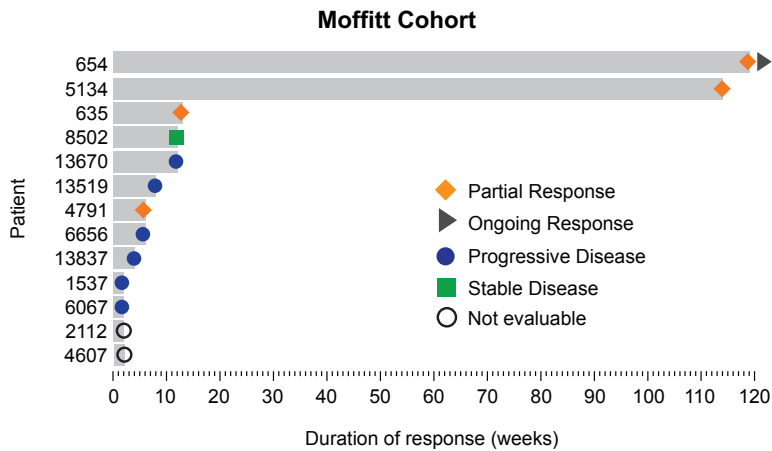


**Figure S5: H&E images of tumors in Rochester validation cohort of relapsed SCLC patients treated with ICB.** Tumor IDs are listed to the left of each H&E image. Scale bars, 100  $\mu$ m. H&Es for 2, 9, 14, 17 and 18 are not shown.

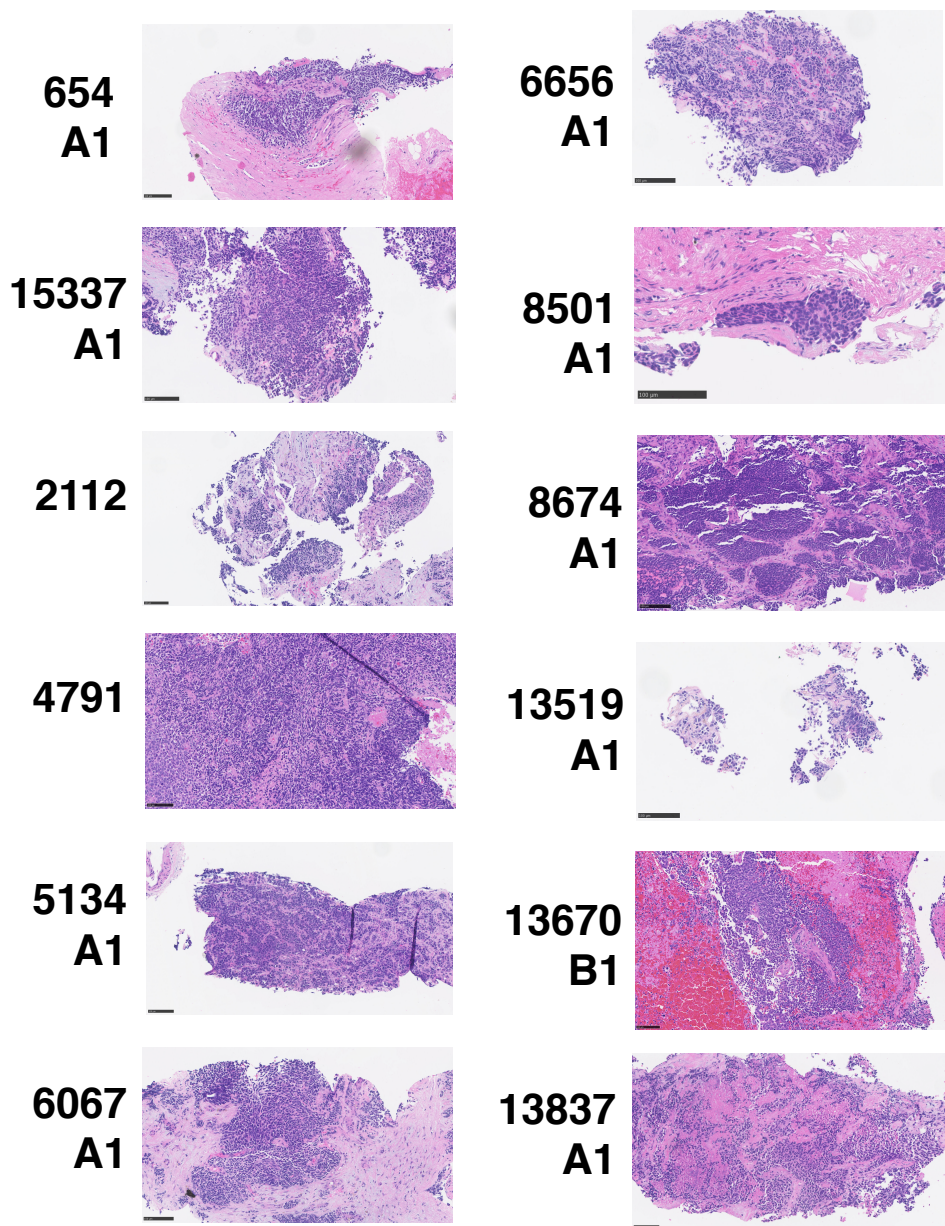


**A****NCI Cohort****B****Rochester Cohort**

**Figure S6: Transcriptional subtypes based on lineage oncogenes of ICB treated SCLC cohorts.** Hierarchical clustering of *ASCL1*, *NEUROD1*, *POU2F3* and *YAP1* gene expression in two ICB treated SCLC cohorts: **(A)** NCI discovery cohort and **(B)** Rochester validation cohort. Relative gene expression is shown (z-score). Red arrows point to tumors from patients who derived clinical benefit to ICB. Source data are provided as a Source Data file.

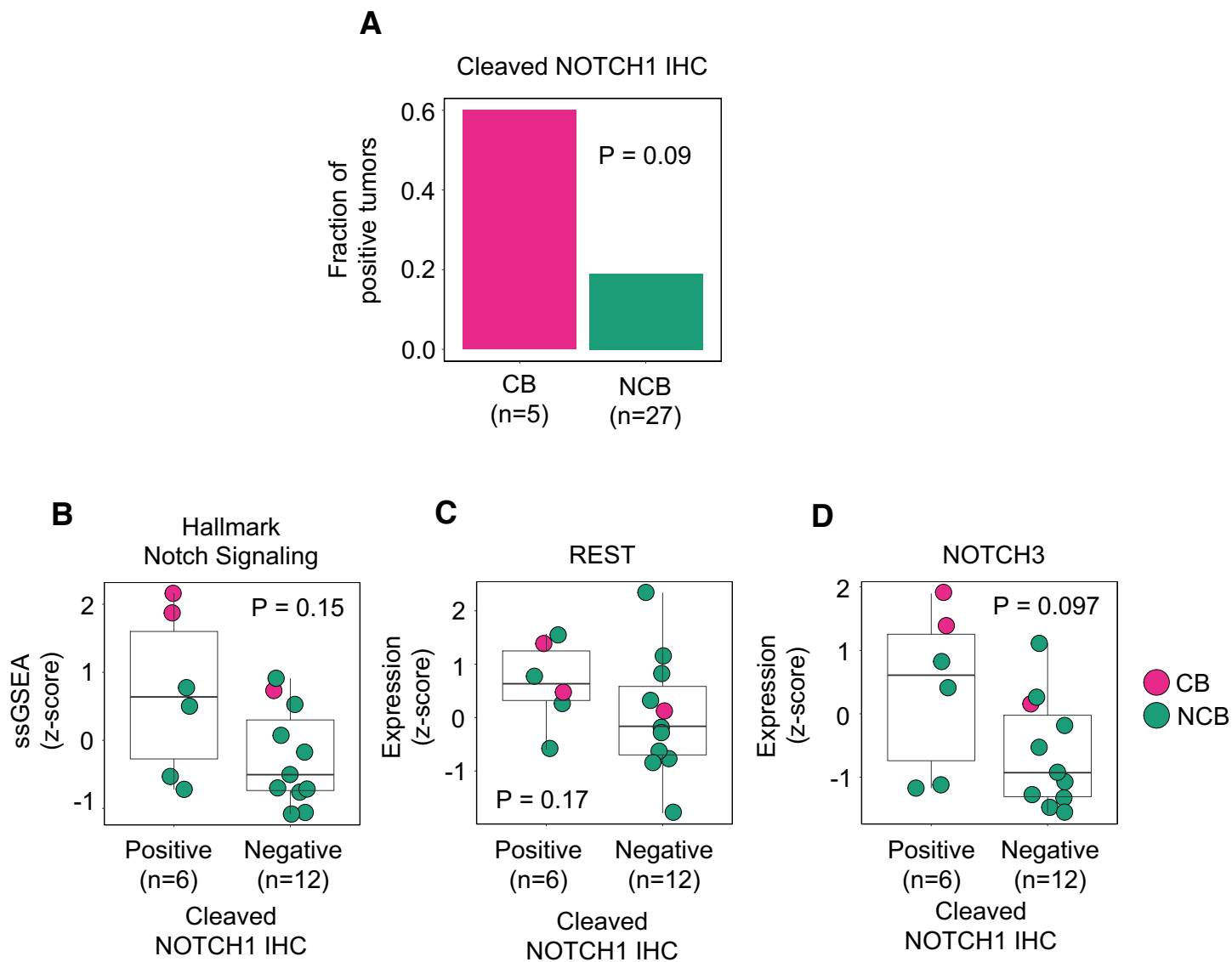
**A****B**

**Figure S7: Flow diagram of samples and clinical responses of patients in Moffitt cohort of relapsed SCLC patients treated with ICB. (A)** Flow diagram of samples in Moffitt Cohort. **(B)** Swimmer's plot indicating response and length of time on therapy for individual patients in the Moffitt cohort. SD: stable disease; PD: progressive disease; PR: partial response; NE: Not evaluable disease



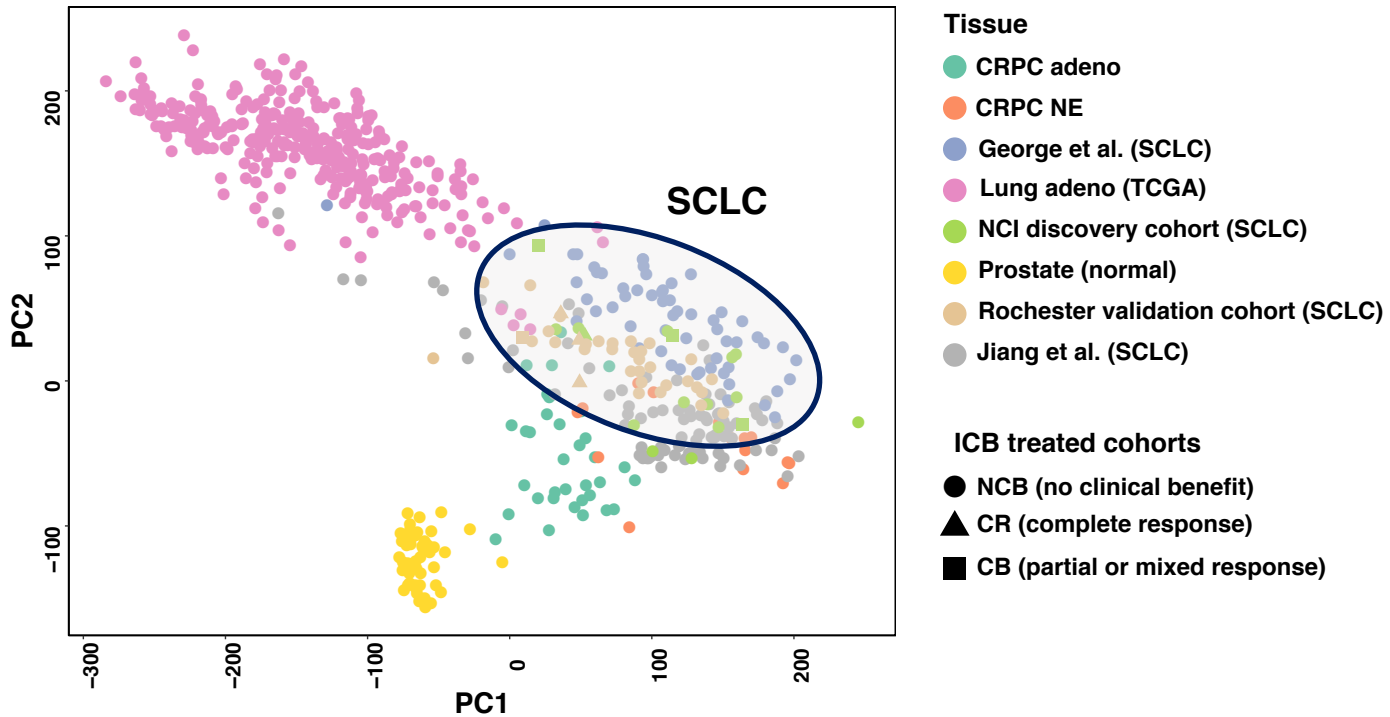
**Figure S8: H&E images of tumors in Moffitt cohort of relapsed SCLC patients treated with ICB.** Tumor IDs are listed to the left of each H&E image. Scale bars, 100  $\mu$ m. H&E for 4607 is not shown.





**Figure S9: Cleaved NOTCH1 immunohistochemistry across ICB treated cohorts of relapsed SCLC.** (A) Fraction of tumors with positive cleaved NOTCH1 IHC (defined as 5% or more positive cells) stratified by CB or NCB to ICB across three ICB-treated cohorts (NCI, Rochester and Moffitt). P-values calculated by Fisher's two-tailed exact test. (B) ssGSEA score for Hallmark Notch signaling, (C) *REST* expression and (D) *NOTCH3* expression of tumors in NCI and Rochester cohorts stratified by positive or negative cleaved NOTCH1 IHC. Statistical significance was tested with a two-tailed Mann–Whitney U-test. Boxplots represent the median, 25th and 75th percentiles and the vertical bars span the 5th to the 95th percentiles. Colored circles represent either CB (pink) or NCB (green) to ICB. CB: clinical benefit; NCB: no clinical benefit. IHC: immunohistochemistry. Source data are provided as a Source Data file.

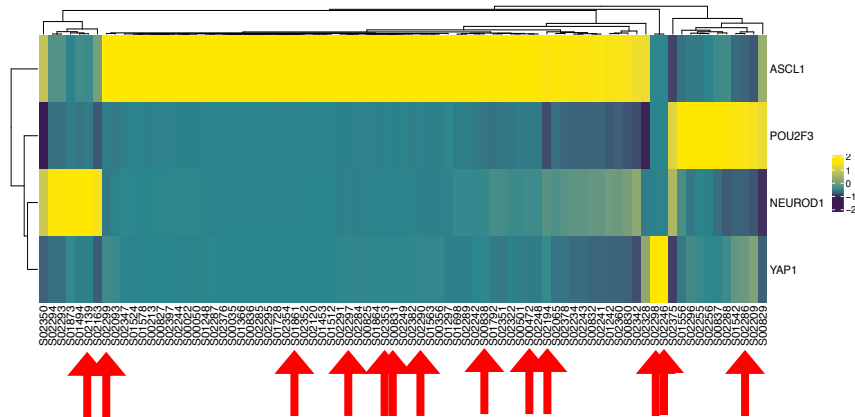
## Principal Component Analysis (Transcriptomic Data)



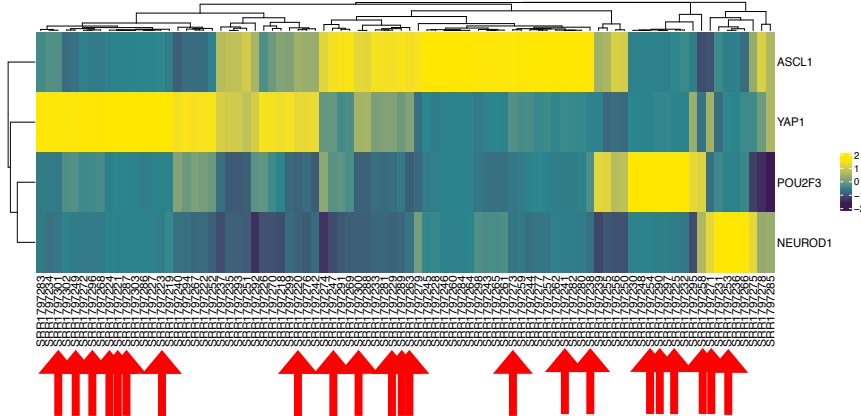
**Figure S10: Transcriptomic relationship between ICB treated SCLC cohorts with previously published non-ICB treated SCLC, lung adenocarcinoma, and prostate cancer cohorts. Ellipse demarcates SCLC tumors from all cohorts. Source data are provided as a Source Data file.**

**A**

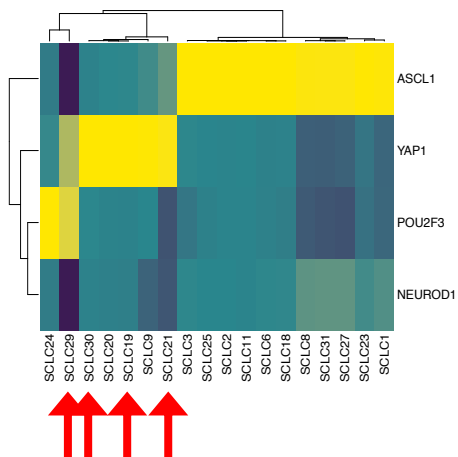
George et al.

**B**

Jiang et al.

**C**

Wagner et al.

**D**

Sato et al.

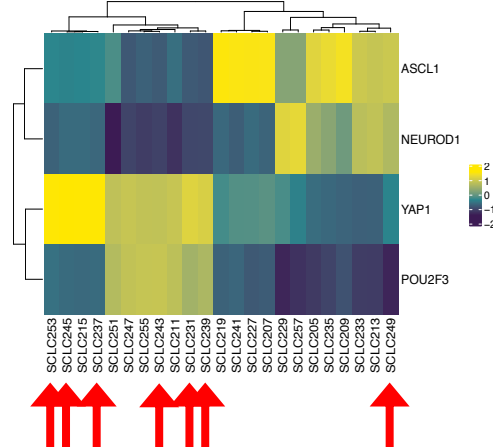


**Figure S11: Transcriptional subtypes based on lineage oncogenes of non-ICB treated SCLC cohorts.** Hierarchical clustering of *ASCL1*, *NEUROD1*, *POU2F3* and *YAP1* gene expression in four small cell lung cancer cohorts without ICB treatment: **(A)** George et al., **(B)** Jiang et al., **(C)** Wagner et. al. and **(D)** Sato et al. Relative gene expression is shown (z-score). Red arrows point to tumors that have high Hallmark Notch gene set expression (Notch<sup>high</sup>). Source data are provided as a Source Data file.



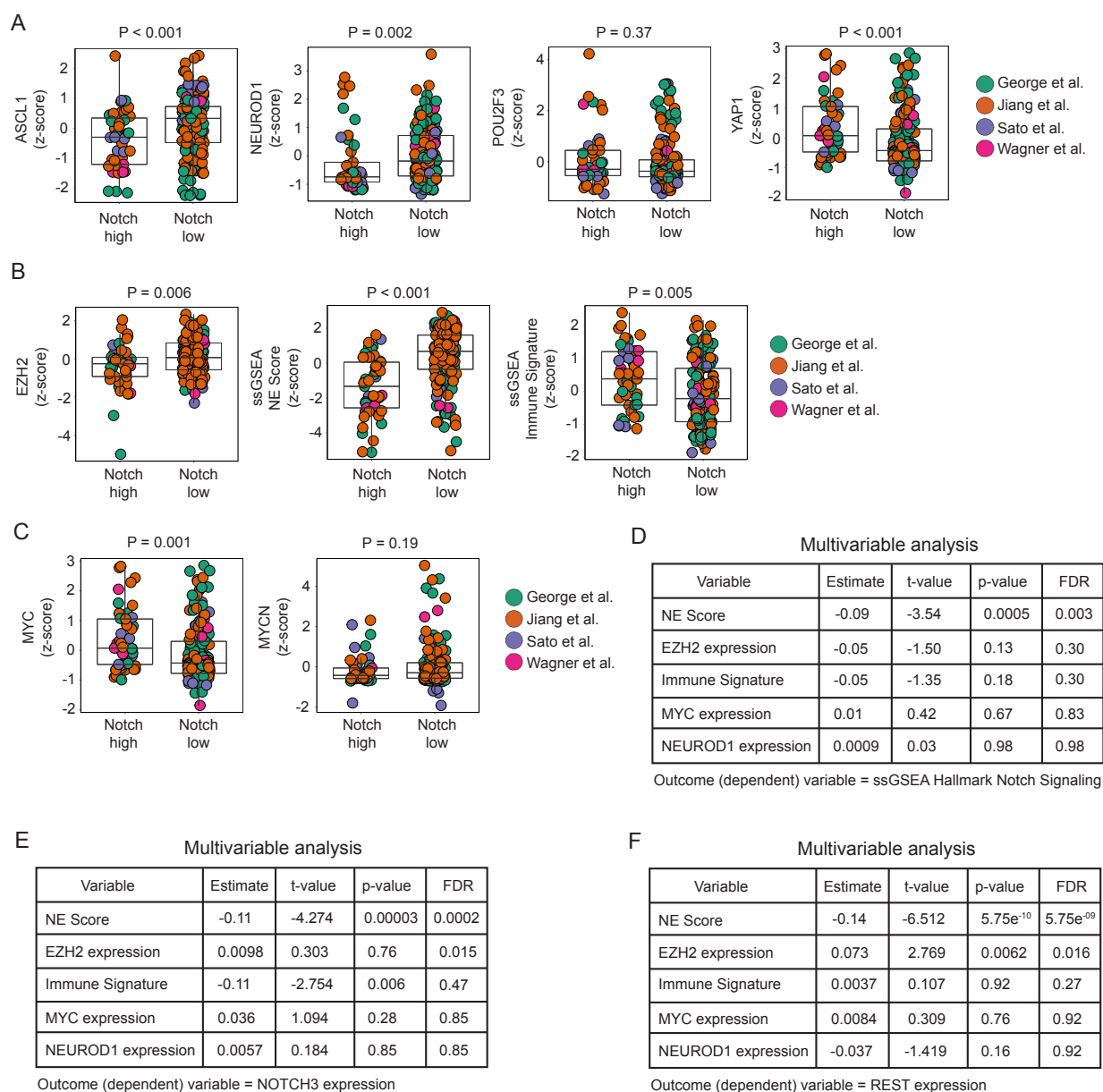


**Figure S12: Notch signaling is significantly associated with neuroendocrine differentiation across non-ICB treated SCLC cohorts.** Association between expression of Hallmark Notch signaling gene set stratified by high (n=45) and low (n=163) and (A) expression of lineage oncogenes *ASCL1*, *NEUROD1*, *POU2F3* and *YAP1*; (B) NE score, expression of immune gene set and expression of *EZH2*; and (C) expression of *MYC* and *MYCN*. (D) Multivariable analysis of variables associated with ssGSEA Hallmark Notch gene set score and with expression of validated Notch signaling target genes (E) *NOTCH3* and (F) *REST*. P-values shown were calculated using a two-tailed Wilcoxon signed-rank test. Linear regression was used for multivariable analysis. False discovery rate was calculated using the Benjamini-Hochberg procedure. Boxplots represent the median, 25th and 75th percentiles and the vertical bars span the 5th to the 95th percentiles. Source data are provided as a Source Data file.

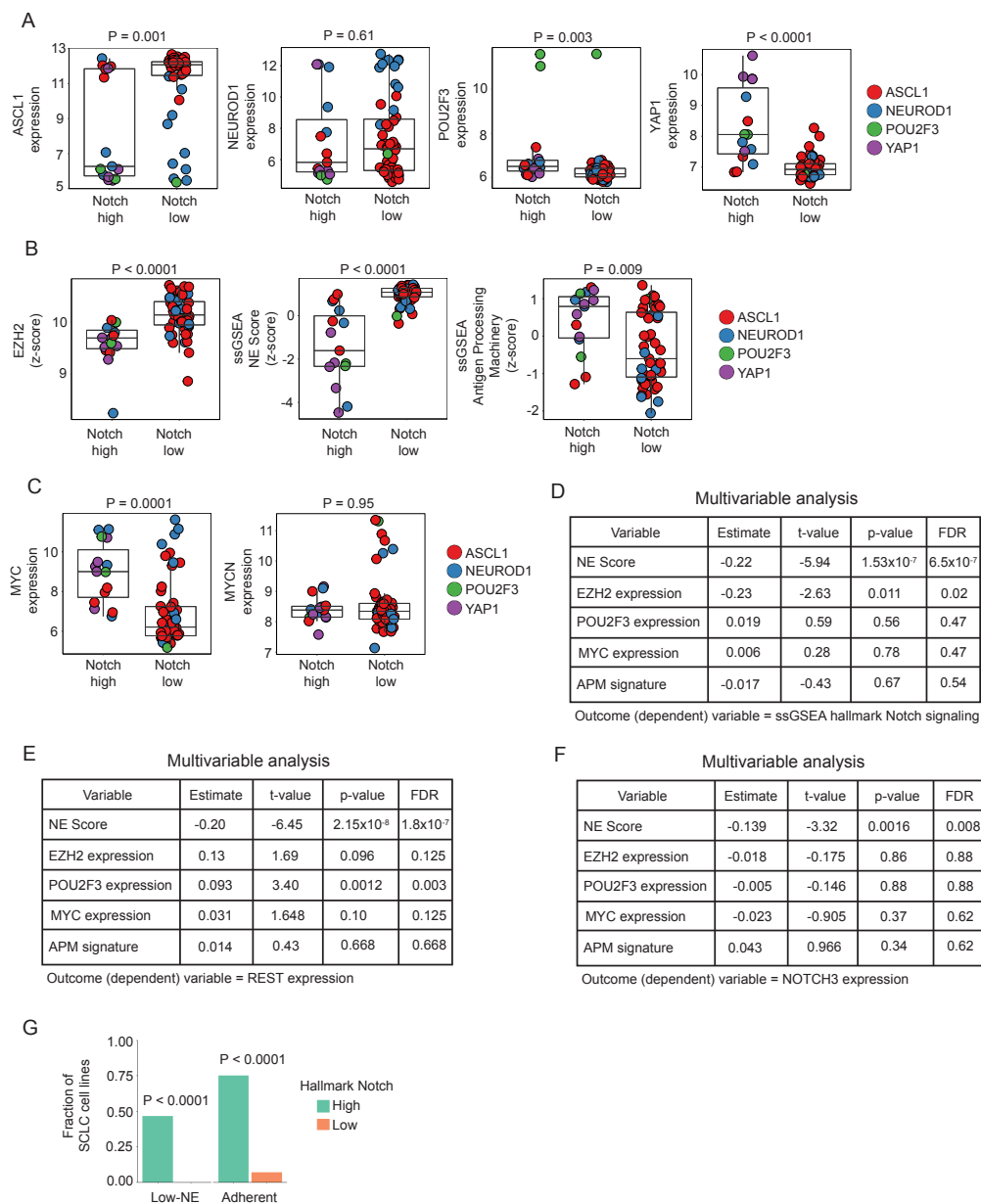


**Figure S13: Notch signaling is significantly associated with neuroendocrine differentiation across SCLC cell lines.** Association between expression of Hallmark Notch signaling gene set stratified by high (n=45) and low (n=163) and (A) expression of lineage oncogenes *ASCL1*, *NEUROD1*, *POU2F3* and *YAP1*; (B) expression of *EZH2*, NE score score, and Antigen Processing Machinery score; and (C) expression of *MYC* and *MYCN*. (D) Multivariable analysis of variables associated with ssGSEA Hallmark Notch gene set score and with expression of validated Notch signaling target genes (E) *NOTCH3* and (F) *REST*. (G) Association between expression of Hallmark Notch signaling gene set (stratified by high and low) with low-NE classification and adherent cell culture properties. P-values shown were calculated using a two-tailed Wilcoxon signed-rank test. Linear regression was used for multivariable analysis. False discovery rate was calculated using the Benjamini-Hochberg procedure. Boxplots represent the median, 25th and 75th percentiles and the vertical bars span the 5th to the 95th percentiles. Source data are provided as a Source Data file.

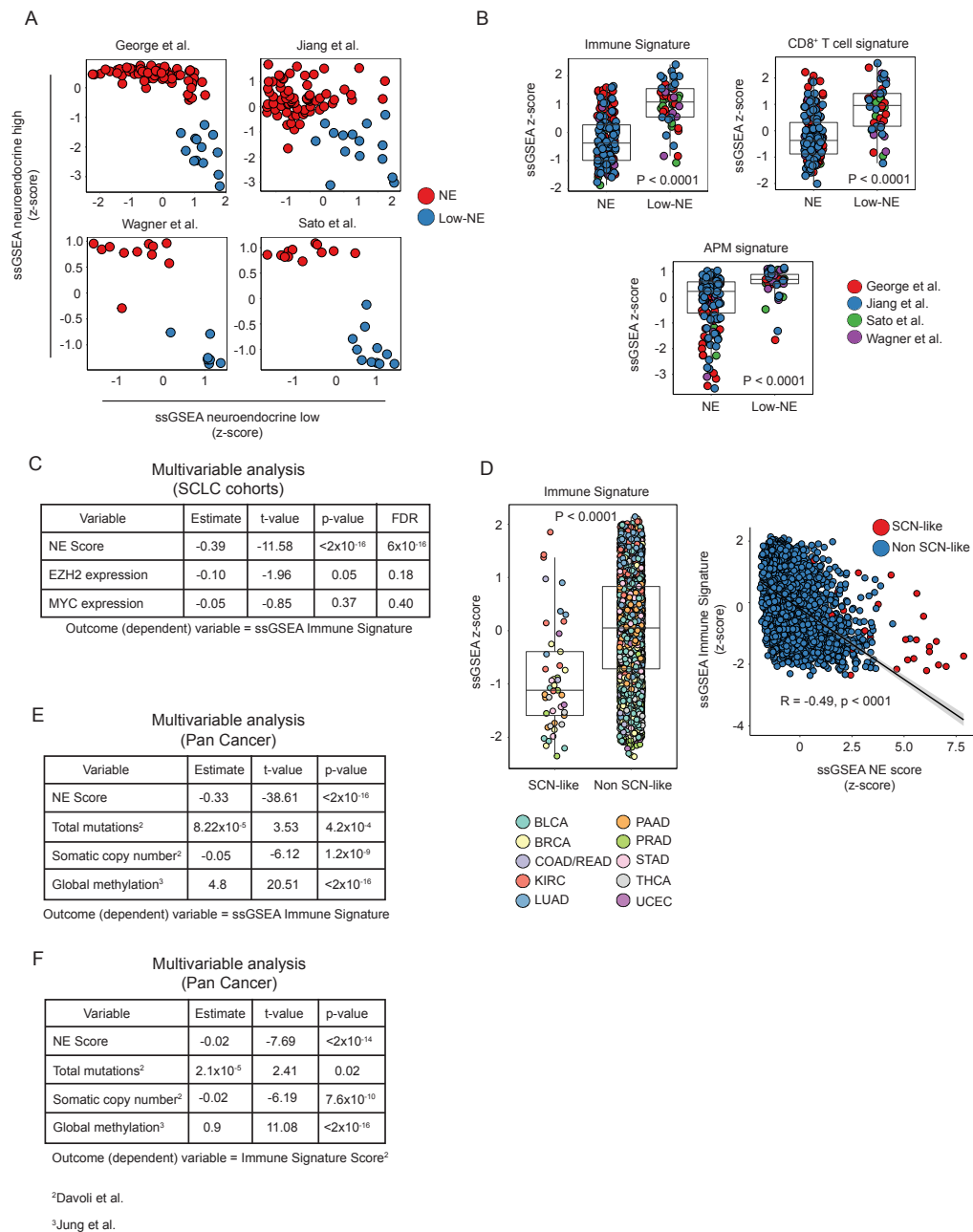


**Figure S14: Neuroendocrine differentiation is significantly associated with expression of immune gene sets in published SCLC cohorts and Pan-Cancer.** (A) Segregation of tumors into NE (n=166) and low-NE (n=42) phenotypes in each of four SCLC cohorts. (B) ssGSEA antigen processing machinery, CD8+ T-cell and immune signature scores in NE and low-NE tumors across the four SCLC cohorts. (C) Multivariable analysis of variables associated with ssGSEA immune signature score across four SCLC cohorts. (D) ssGSEA immune signature score between Pan-Cancer SCN-like (n=45) and non-SCN-like (n=4660) tumors and correlation between ssGSEA NE and ssGSEA immune signature scores. (E and F) Multivariable analysis of factors associated with expression of ssGSEA immune signature score Pan-Cancer. P-values shown were calculated by Wilcoxon signed-rank test. Linear regression was used for multivariable analysis. False discovery rate was calculated using the Benjamini-Hochberg procedure. Boxplots represent the median, 25th and 75th percentiles and the vertical bars span the 5th to the 95th percentiles. Source data are provided as a Source Data file.



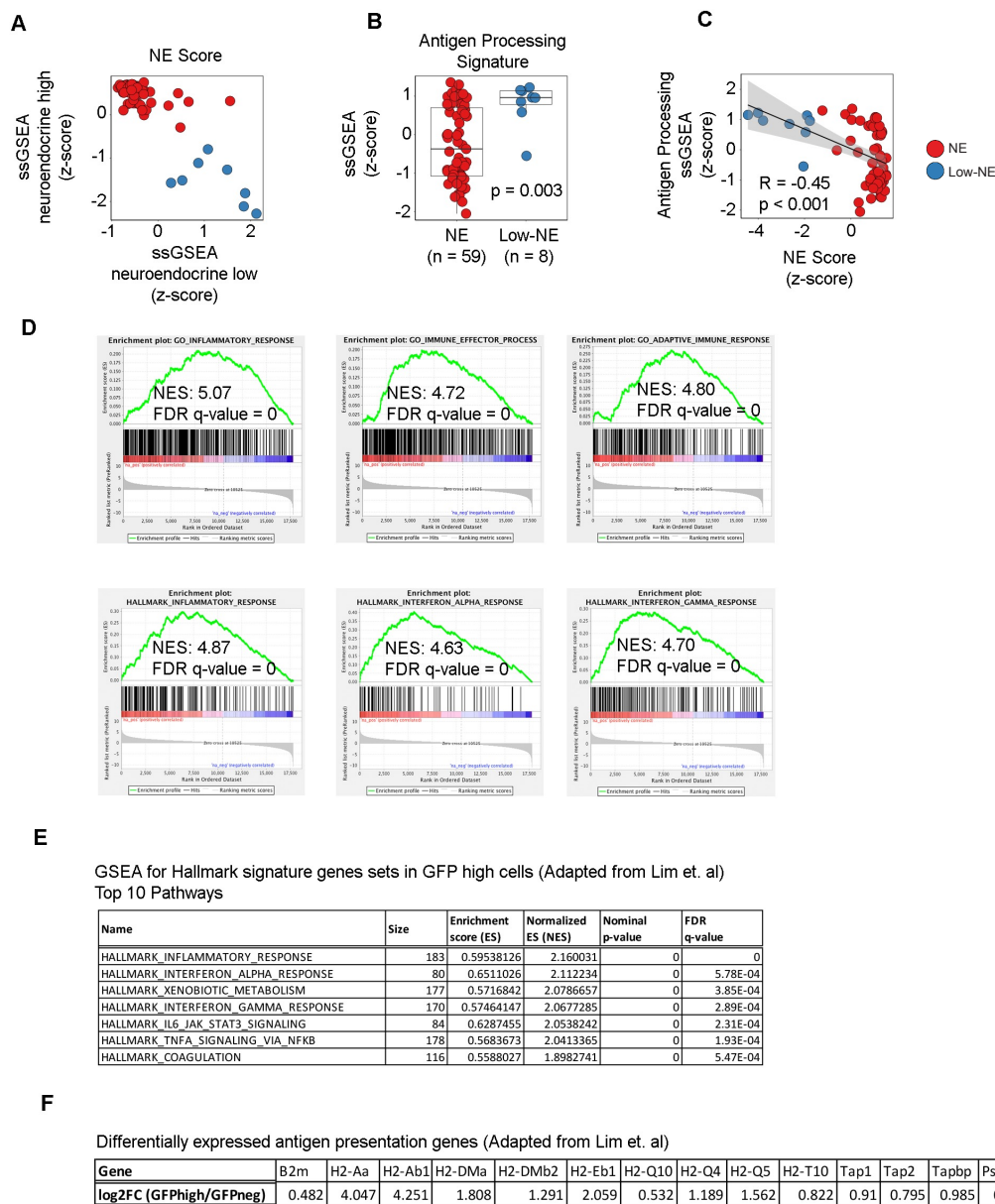


**Figure S15: Enrichment of inflammatory and antigen presentation genes in low-NE SCLC cell lines and a SCLC mouse model. (A)** Segregation of SCLC cell lines into NE (n=59) and low-NE (n=7) phenotypes. **(B)** ssGSEA antigen processing machinery scores in NE and low-NE SCLC cell lines. **(C)** Correlation between ssGSEA antigen processing machinery and NE scores. 95% confidence interval for the line shown in grey shading. **(D)** Significant GSEA enrichment plots comparing low-NE to NE SCLC cell lines. **(E)** Top 10 hallmark pathways enriched in GFP high cells in a mouse model of SCLC. **(F)** Differentially expressed antigen presentation genes in GFP high vs. low cells in a p53<sup>flx/flx</sup>;Rb<sup>flx/flx</sup>;p130<sup>flx/flx</sup> conditional triple knockout (TKO) mouse model of SCLC. Statistical significance was tested with a two-tailed Mann–Whitney U-test. Boxplots represent the median, 25th and 75th percentiles and the vertical bars span the 5th to the 95th percentiles. Source data are provided as a Source Data file.